

# Heterometallic Cu<sub>2</sub>Fe and Zn<sub>2</sub>Fe<sub>2</sub> Complexes Derived from [Fe(CO)<sub>4</sub>]<sup>2−</sup> and Cu/Fe Bifunctional N<sub>2</sub>O Activation Reactivity

Yutthana Lakliang and Neal P. Mankad\*

Cite This: <https://dx.doi.org/10.1021/acs.organomet.0c00212>

Read Online

ACCESS |



Metrics &amp; More

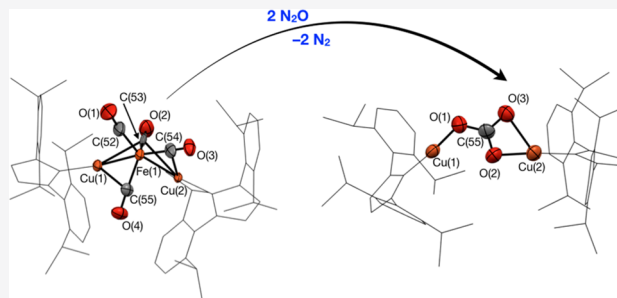


Article Recommendations



Supporting Information

**ABSTRACT:** The synthesis and characterization of two heterometallic clusters, [(IPr)Cu]<sub>2</sub>Fe(CO)<sub>4</sub> (**1**) and [(IPr)ZnFe(CO)<sub>4</sub>]<sub>2</sub> (**2**), derived from Collman's reagent are reported. Methylation of **1** with CH<sub>3</sub>I to produce (IPr)CuI and (IPr)CuFe(Me)(CO)<sub>4</sub> (**3**) was used to calibrate the relative reactivity of **1** to the previously studied analogue (IPr)Cu-FeCp(CO)<sub>2</sub>. Bifunctional N<sub>2</sub>O activation by **1** resulted in oxidation of a CO ligand to carbonate rather than the more typically observed CO<sub>2</sub>, producing [(IPr)Cu]<sub>2</sub>(μ-CO<sub>3</sub>) (**4**) stoichiometrically along with an iron byproduct that was trapped with PPh<sub>3</sub> as *trans*-Fe(CO)<sub>3</sub>(PPh<sub>3</sub>)<sub>2</sub>.



The ongoing effect of climate change motivates the pursuit of technologies that capture<sup>1</sup> greenhouse gases and convert them into useful chemicals or fuels.<sup>2</sup> Achieving such transformations of gaseous small molecules requires catalysts that mediate their efficient activation in order to overcome their thermodynamic stability and/or kinetic inertness.<sup>3</sup> With biological systems as an inspiration, one strategy is to activate inert small molecules using a bifunctional approach, wherein Lewis acidic and basic transition-metal sites cooperate to achieve bond activation. For example, the Ni/Fe cluster of anaerobic carbon monoxide dehydrogenase has been structurally characterized with a bound CO<sub>2</sub> molecule bifunctionally activated by nucleophilic attack at carbon and Lewis acidic stabilization of negative charge accumulation at oxygen.<sup>4</sup> Similarly, N<sub>2</sub>O can be converted to N<sub>2</sub> when it is activated by adjacent Cu sites that act in a bifunctional manner, as seen in the Cu<sub>2</sub> cluster of nitrous oxide reductase or the binuclear active sites of Cu-ZSM-5.<sup>5,6</sup> Mimicking this cooperative strategy for small-molecule activation is currently an active area of research.<sup>7–16</sup>

Previously, our group reported the various heterobimetallic catalyst systems (NHC)M-[M<sub>co</sub>] (NHC = N-heterocyclic carbene; M = Cu, Ag, Au, ZnCl; [M<sub>co</sub>] = e.g. FeCp(CO)<sub>2</sub>, Mn(CO)<sub>5</sub>, WCp(CO)<sub>3</sub>, Co(CO)<sub>4</sub>, etc.), which assemble upon mixing (NHC)MCl and [M<sub>co</sub>]<sup>−</sup> precursors.<sup>17–19</sup> These metal–metal bonds feature polarity that we established through computational methods,<sup>19,20</sup> chemical reactivity,<sup>17,19,21</sup> and spectroscopic analysis.<sup>22</sup> For example, we established that the Cu–Fe bond in (NHC)Cu-Fp (Fp = FeCp(CO)<sub>2</sub>) is polarized: Cu retains positively charged (electrophilic) character, whereas Fe retains negatively charged (nucleophilic) character. This bifunctionality enables cooperative activation of small molecules such as H<sub>2</sub>, CS<sub>2</sub>, and N<sub>2</sub>O under mild conditions.<sup>20,21,23</sup> Additionally, catalyst control over CO<sub>2</sub>

reduction selectively was accomplished with (NHC)Cu-[M] catalysts (M = Fe, W, Mo) when they were activated by a H-[B] reductant.<sup>24</sup> However, we still have not succeeded in bimetallic CO<sub>2</sub> activation using this approach, whereas “early–late” heterobinuclear catalysts that do activate CO<sub>2</sub> using early-transition-metal Lewis acids (e.g., Zr<sup>IV</sup>) are not catalytically active due to the formation of strong metal–oxygen bonds.<sup>7,25,26</sup>

In this context, we hypothesized that the heterobimetallic catalysts might have higher reactivity if the metal–metal bond polarity were further enhanced by replacing monoanionic [M<sub>co</sub>]<sup>−</sup> with a dianionic metal–carbonyl nucleophile. Collman's reagent, Na<sub>2</sub>Fe(CO)<sub>4</sub>, is a well-known compound for organic and organometallic synthesis.<sup>27</sup> Because Collman's reagent features a highly reduced iron formally in its Fe(2−) oxidation state, we hypothesized that its incorporation into heterobimetallic architectures could increase Cu–Fe bond polarity and perhaps enhance reactivity in comparison to (NHC)Cu-Fp derived from [Fp]<sup>−</sup> with a formally Fe(0) center. Herein, we report the synthesis and structural characterization of two new heterometallic complexes, trinuclear [(IPr)Cu]<sub>2</sub>Fe(CO)<sub>4</sub> (**1**) and tetranuclear [(IPr)ZnFe(CO)<sub>4</sub>]<sub>2</sub> (**2**), and the small-molecule activation chemistry of the Cu derivative which can be compared directly to that of its (IPr)CuFp predecessor (IPr = *N,N'*-bis(2,6-diisopropylphenyl)imidazol-2-ylidene). Related complexes

Received: March 27, 2020



such as  $[(\text{Ph}_3\text{P})_2\text{Cu}]_2\text{Fe}(\text{CO})_4$ ,<sup>28</sup>  $[(\text{PPh}_3)\text{Au}_2\text{Fe}(\text{CO})_4]$ ,<sup>29</sup> and  $[(\text{py})_3\text{ZnFe}(\text{CO})_4]$ <sup>30</sup> have been characterized before, but reactivity studies were not performed.

Previously, we reported the syntheses of  $(\text{IPr})\text{CuFp}$  and  $(\text{IPr})(\text{Cl})\text{ZnFp}$  by reactions between  $(\text{IPr})\text{CuCl}$  and  $(\text{IPr})\text{ZnCl}_2(\text{THF})$  synthons and  $\text{KFp}$ .<sup>17</sup> Analogous preparations were used to synthesize **1** and **2** from  $\text{K}_2\text{Fe}(\text{CO})_4$ . The solid-state structure of **1** determined by X-ray crystallography (one of four molecules from the asymmetric unit) is shown in Figure 1a. Unlike  $[(\text{Ph}_3\text{P})\text{Cu}]_2\text{Fe}(\text{CO})_4$ , which features a *trans*

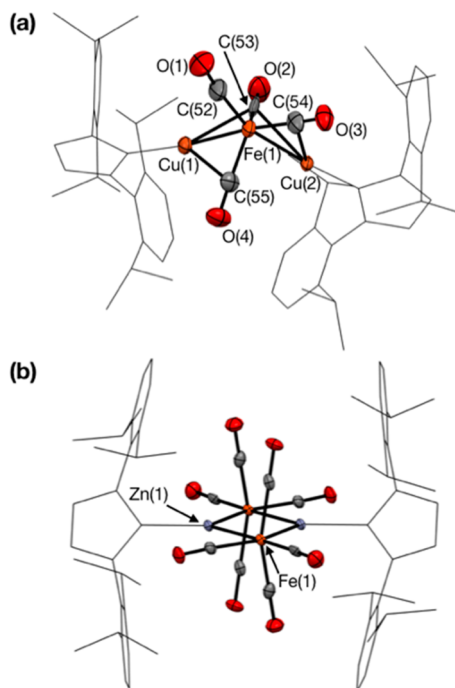


**Figure 1.** Solid-state structures of (a)  $[(\text{IPr})\text{Cu}]_2\text{Fe}(\text{CO})_4$  (**1**) and (b)  $[(\text{IPr})\text{ZnFe}(\text{CO})_4]_2$  (**2**) determined by X-ray crystallography. For clarity, hydrogen atoms and cocrystallized solvent molecules are omitted and NHC ligands are shown as wireframes. All other atoms are shown as 50% probability ellipsoids. For **1**, only one of the four molecules from the asymmetric unit is shown.

orientation of Cu groups ( $168.7(2)^\circ$ ) about an octahedral Fe center,<sup>28</sup> complex **1** features a bent Cu–Fe–Cu angle ( $106.43(5)^\circ$ ) and modestly bent  $\text{C}_{\text{NHC}}\text{--Cu--Fe}$  angles ( $168.1(2)$  and  $172.1(2)^\circ$ ). The Cu–Fe distances ( $2.348(2)$  and  $2.375(1)$  Å) are close to the sum of Pyykkö's single-bond covalent radii of Cu and Fe ( $2.28$  Å)<sup>31</sup> and are among the shortest Cu–Fe distances of any type in Cambridge Structural Database (CSD). The Cu–Fe distances of **1** are similar to that of  $(\text{IPr})\text{Cu--FeCp}(\text{CO})_2$  ( $2.3462(5)$  Å) and slightly longer than the shortest known Cu–Fe distance found in  $(\text{IPr})\text{Cu--FeCp}(\text{CO})(\text{PPh}_2\text{Me})$  ( $2.299(2)$  Å), which presumably has enhanced dative  $\text{Fe}\rightarrow\text{Cu}$  donation due to the electron-donating phosphine ligand.<sup>32</sup> The median Cu–Fe distance in the CSD,  $2.549$  Å, is much longer than the Cu–Fe distances in **1**. The Cu...Cu distance of  $3.783(1)$  Å is too long for a significant interaction. The  $[\text{Fe}(\text{CO})_4]$  unit contained within **1** has a near-perfect tetrahedral arrangement.

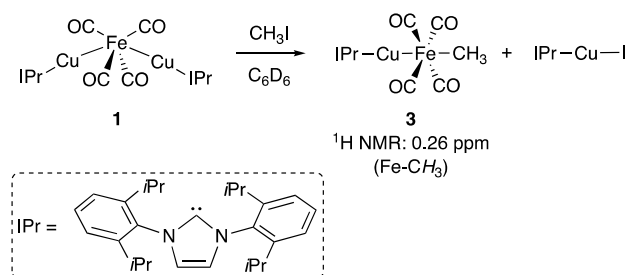
The solid-state structure of **1** contains four independent molecules in the asymmetric unit; only one molecule is discussed here but is representative of the isostructural set. Four short Cu...CO distances are evident: Cu(1)...C(55),

$2.373(7)$  Å; Cu(1)...C(53),  $2.442(6)$  Å; Cu(2)...C(54),  $2.47(1)$  Å; Cu(2)...C(53),  $2.404(8)$  Å. The corresponding asymmetry parameters<sup>33</sup> indicate that all are in the semi-bridging regime.<sup>34</sup> The C(53)–O(2) unit can be considered a semibridging  $\mu_3\text{--CO}$  between Fe(1) and both Cu(1) and Cu(2); the C(53)–O(2) distance of  $1.25(1)$  Å indicates significant CO activation. The C(54)–O(3) and C(55)–O(4) units can be considered semibridging  $\mu_2\text{--CO}$  ligands between Fe(1) and Cu(2) or Cu(1), respectively; the corresponding C–O distances of  $1.194(8)$  and  $1.183(9)$  Å, respectively, indicate weaker activation. The fourth C(52)–O(1) unit is a terminal carbonyl group with a correspondingly short C–O distance of  $1.15(1)$  Å. The solid-state IR spectrum of **1** has a feature at  $1952\text{ cm}^{-1}$  assigned to the terminal CO ligand, features at  $1874$  and  $1833\text{ cm}^{-1}$  assigned to the semibridging  $\mu_2\text{--CO}$  ligands, and a feature at  $1814\text{ cm}^{-1}$  assigned to the more activated  $\mu_3\text{--CO}$  semibridging carbonyl. The  $^{13}\text{C}\{^1\text{H}\}$  NMR spectrum exhibits a single CO resonance at  $216.5$  ppm, indicating that the semibridging interactions are fluxional such that the four CO sites exchange with each other in solution on the NMR time scale.

The solid-state structure of **2** is shown in Figure 1b. Unlike coordinatively saturated, binuclear  $\text{L}_3\text{ZnFe}(\text{CO})_4$  complexes,<sup>30</sup> the unsaturated “ $(\text{IPr})\text{ZnFe}(\text{CO})_4$ ” species in **2** apparently dimerizes to form tetranuclear  $[(\text{IPr})\text{ZnFe}(\text{CO})_4]_2$ . The Zn–Fe distances in **2** of  $2.5221(7)$  and  $2.5293(8)$  Å are much longer than that in  $(\text{IPr})(\text{Cl})\text{Zn--FeCp}(\text{CO})_2$  ( $2.3714(4)$  Å).<sup>17</sup> To compare the M–Fe distances, Cotton's formal shortness ratio (FSR) calculations can be used to correct for metal sizes.<sup>35</sup> The average FSR value for Cu–Fe in **1** ( $1.004$ ) is smaller than that for Zn–Fe in **2** ( $1.048$ ), which might be due to the differences in Pauling's atomic radii for Cu ( $1.73$  Å) and Zn ( $1.249$  Å).<sup>36</sup> The Fe centers in **2** have nearly ideal octahedral environments, possibly due to the lack of any close Zn...CO contacts to create structural distortions as in **1**. The cross-cluster Fe...Fe ( $4.196(1)$  Å) and Zn...Zn ( $2.8124(5)$  Å) distances are too long for any significant interaction.

We have begun to benchmark the reactivity of these new clusters using reactions for which **1** can be compared directly to its  $(\text{IPr})\text{CuFp}$  analogue. We initially established the Cu–Fe bond polarity of  $(\text{IPr})\text{CuFp}$  through its reactivity with methyl iodide.<sup>17,22</sup> Similarly, here complex **1** was exposed to equimolar  $\text{CH}_3\text{I}$ . An analysis of the product mixture by  $^1\text{H}$  NMR indicated quantitative formation of  $(\text{IPr})\text{CuI}$  and a second species assigned as  $(\text{IPr})\text{CuFe}(\text{Me})(\text{CO})_4$  (**3**) (Scheme 1). No evidence for  $(\text{IPr})\text{CuCH}_3$  or  $\text{I}_2\text{Fe}(\text{CO})_4$  was detected, consistent with the proposed Cu–Fe bond polarity of formally Cu(I) Lewis acidic and Fe(2–) Lewis basic sites. Exposure of the product mixture to additional  $\text{CH}_3\text{I}$  did not result in any further conversion of **3** to  $(\text{IPr})\text{CuI}$ . Because we initially

### Scheme 1. Methyl Iodide Reactivity of **1**



hypothesized that **1** would have more reactive Cu–Fe bonds than (IPr)CuFp, we sought to measure rate constants under pseudo-first-order conditions (excess CH<sub>3</sub>I), using <sup>1</sup>H NMR to monitor the appearance of Fe–CH<sub>3</sub> resonances. The observed rate constants at room temperature for **1** and (IPr)CuFp were 0.028 and 0.041 s<sup>−1</sup>, respectively. In other words, in contrast to our initial hypothesis, the two complexes are about equally reactive toward CH<sub>3</sub>I within error. This result highlights the limitations of formal oxidation states in predicting reactivity behavior.<sup>37</sup>

We previously reported that exposure of (NHC)CuFp derivatives to N<sub>2</sub>O results in Cp<sup>−</sup> migration from Fe to Cu, producing (NHC)CuCp products quantitatively with precipitation of an amorphous Fe<sub>x</sub>C<sub>y</sub>O<sub>z</sub> material.<sup>21</sup> Thus, we were curious to examine the behavior toward N<sub>2</sub>O of complex **1**, which lacks a Cp<sup>−</sup> group. Stirring a solution of **1** in toluene under N<sub>2</sub>O (1 atm) at room temperature caused rapid precipitation of a dark brown material. Analysis of the soluble fraction by <sup>1</sup>H NMR spectroscopy indicated the formation of a single product, which was determined to be the carbonate complex [(IPr)Cu]<sub>2</sub>(μ-CO<sub>3</sub>) (**4**) by X-ray crystallography. The solid-state structure of **4** (Figure 2) shows a bridging μ-

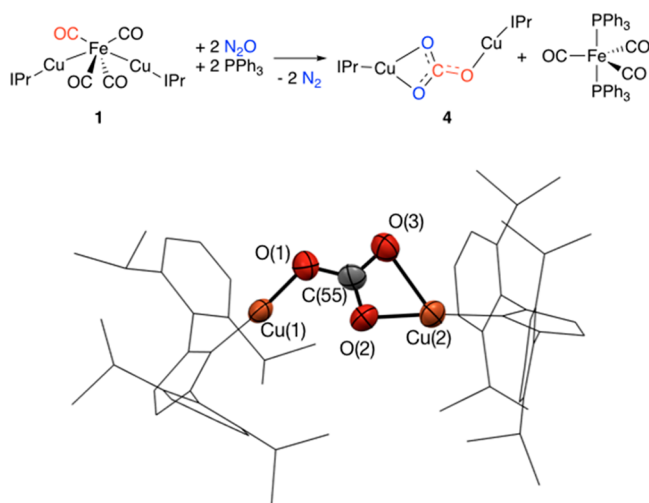


**Figure 2.** Stoichiometry of N<sub>2</sub>O activation by **1** (top) and solid-state structure of [(IPr)Cu]<sub>2</sub>(μ-CO<sub>3</sub>) (**4**; bottom).

carbonate ligand that binds in a κ<sup>1</sup> mode through O(1) to Cu(1) and a κ<sup>2</sup> mode through O(2) and O(3) to Cu(2). The dark brown precipitate forming alongside **4** did not dissolve in any common organic solvents, but on the basis of the reaction stoichiometry it is expected to be 1/*n*[Fe(CO)<sub>3</sub>]<sub>*n*</sub>. Accordingly, this byproduct could be solubilized by trapping with a phosphine ligand. Exposure of **1** to N<sub>2</sub>O (1 atm) in the presence of PPh<sub>3</sub> (3 equiv) produced *trans*-Fe(CO)<sub>3</sub>(PPh<sub>3</sub>)<sub>2</sub> along with OPPh<sub>3</sub> (0.04 equiv). The generation of *trans*-Fe(CO)<sub>3</sub>(PPh<sub>3</sub>)<sub>2</sub> was confirmed by <sup>31</sup>P NMR spectroscopy as well as comparison of X-ray diffraction data to literature reports.<sup>38</sup> Independently, triphenylphosphine was found to be unreactive toward both **1** and N<sub>2</sub>O individually under these conditions. The overall balanced reaction (Figure 2) involves a single CO ligand being oxidized to [CO<sub>3</sub>]<sup>2−</sup> by 2 equiv of N<sub>2</sub>O. Although metal catalysts are known to mediate oxygen atom transfer from N<sub>2</sub>O to CO to generate CO<sub>2</sub>,<sup>39,40</sup> including in automobile catalytic converters,<sup>41</sup> to our knowledge the production of [CO<sub>3</sub>]<sup>2−</sup> has not been reported before.

No reaction between **1** and CO<sub>2</sub> (1 atm) in C<sub>6</sub>D<sub>6</sub> at room temperature was observed from <sup>1</sup>H NMR spectral data. Use of isotopically enriched <sup>13</sup>CO<sub>2</sub> further indicated that no equilibration was occurring between carbon dioxide and the carbonyl groups, as has been observed in some early–late heterobimetallic systems.<sup>25</sup> Further work on activation of CO<sub>2</sub> and other small molecules by **1** and **2** is ongoing in our laboratories.

## ■ ASSOCIATED CONTENT

### Supporting Information

The Supporting Information is available free of charge at <https://pubs.acs.org/doi/10.1021/acs.organomet.0c00212>.

Experimental procedures and spectral data (PDF)

### Accession Codes

CCDC 1985380–1985382 contain the supplementary crystallographic data for this paper. These data can be obtained free of charge via [www.ccdc.cam.ac.uk/data\\_request/cif](http://www.ccdc.cam.ac.uk/data_request/cif), or by emailing [data\\_request@ccdc.cam.ac.uk](mailto:data_request@ccdc.cam.ac.uk), or by contacting The Cambridge Crystallographic Data Centre, 12 Union Road, Cambridge CB2 1EZ, UK; fax: +44 1223 336033.

## ■ AUTHOR INFORMATION

### Corresponding Author

Neal P. Mankad – Department of Chemistry, University of Illinois at Chicago, Chicago, Illinois 60607, United States; [orcid.org/0000-0001-6923-5164](https://orcid.org/0000-0001-6923-5164); Email: [npm@uic.edu](mailto:npm@uic.edu)

### Author

Yutthana Lakliang – Department of Chemistry, University of Illinois at Chicago, Chicago, Illinois 60607, United States

Complete contact information is available at:

<https://pubs.acs.org/doi/10.1021/acs.organomet.0c00212>

### Notes

The authors declare no competing financial interest.

## ■ ACKNOWLEDGMENTS

Funding for this study was provided by the NSF (CHE-1664632).

## ■ REFERENCES

- (1) Boot-Handford, M. E.; Abanades, J. C.; Anthony, E. J.; Blunt, M. J.; Brandani, S.; Mac Dowell, N.; Fernández, J. R.; Ferrari, M. C.; Gross, R.; Hallett, J. P.; Haszeldine, R. S.; Heptonstall, P.; Lyngfelt, A.; Makuch, Z.; Mangano, E.; Porter, R. T. J.; Mourkashanian, M.; Rochelle, G. T.; Shah, N.; Yao, J. G.; Fennell, P. S. Carbon Capture and Storage Update. *Energy Environ. Sci.* **2014**, *7*, 130–189.
- (2) Tappe, N. A.; Reich, R. M.; D'Elia, V.; Kühn, F. E. Current Advances in the Catalytic Conversion of Carbon Dioxide by Molecular Catalysts: An Update. *Dalton Trans.* **2018**, *47*, 13281–13313.
- (3) Kokoja, M.; Bruckmeier, C.; Rieger, B.; Herrmann, W. A.; Kühn, F. E. Transformation of Carbon Dioxide with Homogeneous Transition-Metal Catalysts: A Molecular Solution to a Global Challenge? *Angew. Chem., Int. Ed.* **2011**, *50*, 8510–8537.
- (4) Jeoung, J. H.; Dobbek, H. Carbon Dioxide Activation at the Ni<sub>2</sub>Fe-Cluster of Anaerobic Carbon Monoxide Dehydrogenase. *Science* **2007**, *318*, 1461–1464.
- (5) Johnston, E. M.; Carreira, C.; Dell'Acqua, S.; Dey, S. G.; Pauleta, S. R.; Moura, I.; Solomon, E. I. Spectroscopic Definition of the CuZ<sup>0</sup> Intermediate in Turnover of Nitrous Oxide Reductase and Molecular Insight into the Catalytic Mechanism. *J. Am. Chem. Soc.* **2017**, *139*, 4462–4476.



- (6) Tsai, M.-L.; Hadt, R. G.; Vanelderen, P.; Sels, B. F.; Schoonheydt, R. A.; Solomon, E. I.  $[\text{Cu}_2\text{O}]^{2+}$  Active Site Formation in Cu-ZSM-5: Geometric and Electronic Structure Requirements for  $\text{N}_2\text{O}$  Activation. *J. Am. Chem. Soc.* **2014**, *136*, 3522–3529.
- (7) Krogman, J. P.; Foxman, B. M.; Thomas, C. M. Activation of  $\text{CO}_2$  by a Heterobimetallic Zr/Co Complex. *J. Am. Chem. Soc.* **2011**, *133*, 14582–14585.
- (8) Cammarota, R. C.; Clouston, L. J.; Lu, C. C. Leveraging Molecular Metal–Support Interactions for  $\text{H}_2$  and  $\text{N}_2$  Activation. *Coord. Chem. Rev.* **2017**, *334*, 100–111.
- (9) Campos, J. Dihydrogen and Acetylene Activation by a Gold(I)/Platinum(0) Transition Metal Only Frustrated Lewis Pair. *J. Am. Chem. Soc.* **2017**, *139*, 2944–2947.
- (10) Hollingsworth, T. S.; Hollingsworth, R. L.; Lord, R. L.; Groysman, S. Cooperative Bimetallic Reactivity of a Heterodinuclear Molybdenum–Copper Model of Mo–Cu CODH. *Dalton Trans.* **2018**, *47* (30), 10017–10024.
- (11) Uyeda, C.; Peters, J. C. Selective Nitrite Reduction at Heterobimetallic CoMg Complexes. *J. Am. Chem. Soc.* **2013**, *135*, 12023–12031.
- (12) Steiman, T. J.; Uyeda, C. Reversible Substrate Activation and Catalysis at an Intact Metal–Metal Bond Using a Redox-Active Supporting Ligand. *J. Am. Chem. Soc.* **2015**, *137*, 6104–6110.
- (13) Cooper, O.; Camp, C.; Pécaut, J.; Kefalidis, C. E.; Maron, L.; Gambarelli, S.; Mazzanti, M. Multimetallic Cooperativity in Uranium-Mediated  $\text{CO}_2$  Activation. *J. Am. Chem. Soc.* **2014**, *136*, 6716–6723.
- (14) Hicken, A.; White, A. J. P.; Crimmin, M. R. Selective Reduction of  $\text{CO}_2$  to a Formate Equivalent with Heterobimetallic Gold–Copper Hydride Complexes. *Angew. Chem., Int. Ed.* **2017**, *56*, 15127–15130.
- (15) Powers, T. M.; Betley, T. A. Testing the Polynuclear Hypothesis: Multielectron Reduction of Small Molecules by Triiron Reaction Sites. *J. Am. Chem. Soc.* **2013**, *135*, 12289–12296.
- (16) Velian, A.; Lin, S.; Miller, A. J. M.; Day, M. W.; Agapie, T. Synthesis and C–C Coupling Reactivity of a Dinuclear Ni I–Ni I Complex Supported by a Terphenyl Diphosphine. *J. Am. Chem. Soc.* **2010**, *132*, 6296–6297.
- (17) Jayarathne, U.; Mazzacano, T. J.; Bagherzadeh, S.; Mankad, N. P. Heterobimetallic Complexes with Polar, Unsupported Cu–Fe and Zn–Fe Bonds Stabilized by N-Heterocyclic Carbenes. *Organometallics* **2013**, *32*, 3986–3992.
- (18) Banerjee, S.; Karunananda, M. K.; Bagherzadeh, S.; Jayarathne, U.; Parmelee, S. R.; Waldhart, G. W.; Mankad, N. P. Synthesis and Characterization of Heterobimetallic Complexes with Direct Cu–M Bonds (M = Cr, Mn, Co, Mo, Ru, W) Supported by N-Heterocyclic Carbene Ligands: A Toolkit for Catalytic Reaction Discovery. *Inorg. Chem.* **2014**, *53*, 11307–11315.
- (19) Karunananda, M. K.; Parmelee, S. R.; Waldhart, G. W.; Mankad, N. P. Experimental and Computational Characterization of the Transition State for C–X Bimetallic Oxidative Addition at a Cu–Fe Reaction Center. *Organometallics* **2015**, *34*, 3857–3864.
- (20) Karunananda, M. K.; Mankad, N. P. Heterobimetallic H<sub>2</sub> Addition and Alkene/Alkane Elimination Reactions Related to the Mechanism of E-Selective Alkyne Semihydrogenation. *Organometallics* **2017**, *36*, 220–227.
- (21) Jayarathne, U.; Parmelee, S. R.; Mankad, N. P. Small Molecule Activation Chemistry of Cu–Fe Heterobimetallic Complexes Toward  $\text{CS}_2$  and  $\text{N}_2\text{O}$ . *Inorg. Chem.* **2014**, *53*, 7730–7737.
- (22) Karunananda, M. K.; Vázquez, F. X.; Alp, E. E.; Bi, W.; Chattopadhyay, S.; Shibata, T.; Mankad, N. P. Experimental Determination of Redox Cooperativity and Electronic Structures in Catalytically Active Cu–Fe and Zn–Fe Heterobimetallic Complexes. *Dalton Trans.* **2014**, *43*, 13661.
- (23) Karunananda, M. K.; Mankad, N. P. E-Selective Semihydrogenation of Alkynes by Heterobimetallic Catalysis. *J. Am. Chem. Soc.* **2015**, *137*, 14598–14601.
- (24) Bagherzadeh, S.; Mankad, N. P. Catalyst Control of Selectivity in  $\text{CO}_2$  Reduction Using a Tunable Heterobimetallic Effect. *J. Am. Chem. Soc.* **2015**, *137*, 10898–10901.
- (25) Pinkes, J. R.; Steffey, B. D.; Vites, J. C.; Cutler, A. R. Carbon Dioxide Insertion into the Fe–Zr and Ru–Zr Bonds of the Heterobimetallic Complexes  $\text{Cp}(\text{CO})_2\text{M–Zr}(\text{Cl})\text{Cp}_2$ : Direct Production of the  $\mu\text{-}\eta^1(\text{C})\text{:}\eta^2(\text{O},\text{O}')\text{-CO}_2$  Compounds  $\text{Cp}(\text{CO})_2\text{M–CO}_2\text{-Zr}(\text{Cl})\text{Cp}_2$ . *Organometallics* **1994**, *13*, 21–23.
- (26) Hanna, T. A.; Baranger, A. M.; Bergman, R. G. Reaction of Carbon Dioxide and Heterocumulenes with an Unsymmetrical Metal–Metal Bond. Direct Addition of Carbon Dioxide across a Zirconium–Iridium Bond and Stoichiometric Reduction of Carbon Dioxide to Formate. *J. Am. Chem. Soc.* **1995**, *117*, 11363–11364.
- (27) Collman, J. P.; Colman, J. P. Disodium Tetracarbonylferrate, a Transition Metal Analog of a Grignard Reagent. *Acc. Chem. Res.* **1975**, *8*, 342–347.
- (28) Doyle, G.; Eriksen, K. A.; Van Engen, D. Mixed Copper/Iron Clusters. The Preparation and Structures of  $[(\text{Ph}_3\text{P})_2\text{Cu}]_2\text{Fe}(\text{CO})_4$  and  $[(\text{Diphos})_2\text{Cu}]_2\text{Cu}_6\text{Fe}_4(\text{CO})_{16}$ . *J. Am. Chem. Soc.* **1985**, *107*, 7914–7920.
- (29) Bortoluzzi, M.; Cesari, C.; Ciabatti, I.; Femoni, C.; Hayatifar, M.; Iapalucci, M. C.; Mazzoni, R.; Zacchini, S. Bimetallic Fe–Au Carbonyl Clusters Derived from Collman’s Reagent: Synthesis, Structure and DFT Analysis of  $\text{Fe}(\text{CO})_4(\text{AuNHC})_2$  and  $[\text{Au}_3\text{Fe}_2(\text{CO})_8(\text{NHC})_2]^-$ . *J. Cluster Sci.* **2017**, *28*, 703–723.
- (30) Ernst, R. D.; Marks, T. J. Chemical and Structural Relationships among the Oligomeric Compounds  $\text{MFe}(\text{CO})_4$  (M = Zn, Cd, Hg),  $\text{PbFe}(\text{CO})_4$ ,  $\text{AgCo}(\text{CO})_4$ , and Their Base Adducts. *Inorg. Chem.* **1978**, *17*, 1477.
- (31) Pyykkö, P.; Atsumi, M. Molecular Single-Bond Covalent Radii for Elements 1–118. *Chem. - Eur. J.* **2009**, *15*, 186–197.
- (32) Leon, N. J.; Yu, H.-C.; Mazzacano, T. J.; Mankad, N. P. Mixed Phosphine/Carbonyl Derivatives of Heterobimetallic Copper–Iron and Copper–Tungsten Catalysts. *Polyhedron* **2019**, *157*, 116–123.
- (33) Curtis, M. D.; Han, K. R.; Butler, W. M. Metal–Metal Multiple Bonds. 5. Molecular Structure and Fluxional Behavior of Tetraethylammonium.  $\mu\text{-Cyano-Bis}$  (Cyclopentadienyldicarbonylmolybdate)–(Mo–Mo) and the Question of Semibridging Carbonyls. *Inorg. Chem.* **1980**, *19*, 2096–2101.
- (34) Parmelee, S. R.; Mankad, N. P. A Data-Intensive Re-Evaluation of Semibridging Carbonyl Ligands. *Dalton Trans.* **2015**, *44*, 17007–17014.
- (35) Cotton, F. A.; Daniels, L. M.; Murillo, C. A.; Zhou, H. C. The Effect of Divergent-Bite Ligands on Metal–Metal Bond Distances in Some Paddlewheel Complexes. *Inorg. Chim. Acta* **2000**, *300*–302, 319–327.
- (36) Pauling, L. Atomic Radii and Interatomic Distances in Metals. *J. Am. Chem. Soc.* **1947**, *69*, 542–553.
- (37) Wolczanski, P. T. Flipping the Oxidation State Formalism: Charge Distribution in Organometallic Complexes As Reported by Carbon Monoxide. *Organometallics* **2017**, *36*, 622–631.
- (38) Glaser, R.; Yoo, Y.-H.; Chen, G. S.; Barnes, C. L. Crystal Structure of *Trans*- $\text{Fe}(\text{CO})_3(\text{PPh}_3)_2$ , Tricarbonylbis-(Triphenylphosphine)Iron(0), and *Ab Initio* Study of the Bonding in *Trans*- $\text{Fe}(\text{CO})_3(\text{PH}_3)_2$ . *Organometallics* **1994**, *13*, 2578–2586.
- (39) Yonke, B. L.; Reeds, J. P.; Zavalij, P. Y.; Sita, L. R. Catalytic Degenerate and Nondegenerate Oxygen Atom Transfers Employing  $\text{N}_2\text{O}$  and  $\text{CO}_2$  and a  $\text{M}^{\text{II}}/\text{M}^{\text{IV}}$  Cycle Mediated by Group 6  $\text{M}^{\text{IV}}$  Terminal Oxo Complexes. *Angew. Chem., Int. Ed.* **2011**, *50*, 12342–12346.
- (40) Hartmann, N. J.; Wu, G.; Hayton, T. W. Synthesis and Reactivity of a Nickel(II) Thioperoxide Complex: Demonstration of Sulfide-Mediated  $\text{N}_2\text{O}$  Reduction. *Chem. Sci.* **2018**, *9*, 6580–6588.
- (41) Granger, P.; Parvulescu, V. I. Catalytic  $\text{NO}_x$  Abatement Systems for Mobile Sources: From Three-Way to Lean Burn after-Treatment Technologies. *Chem. Rev.* **2011**, *111*, 3155–3207.